Recommendations on the most reliable predictor variables and evaluation of inter-relationships

Jürg Schmidli

ETH partner report for deliverable D13 — 2 Dec 2004

Atmospheric and Climate Sciences, ETH Zürich, Switzerland

Introduction

The purpose of deliverable D13 is to evaluate the reliability of the GCM simulated predictors. Our downscaling method requires large-scale precipitation and the leading few principal components of the geopotential height field. The present report focusses on our specific predictor, the GCM simulated precipitation. Thus the precipitation simulated by HadAM3P is evaluated.

Data and method

We evaluate the HadAM precipitation for the European sector and in more detail for the twelve HadAM grid points located in the Alpine region (Fig. 1). The evaluation is based on the following

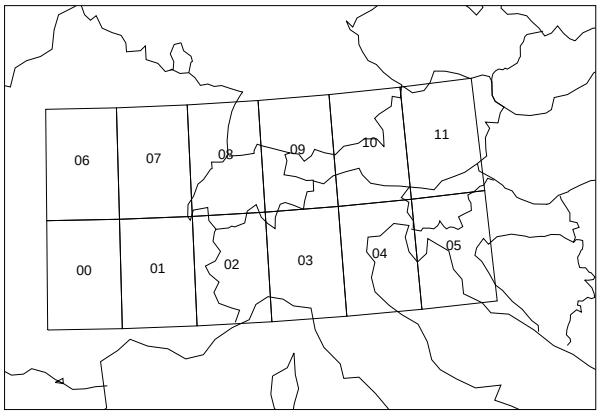

Figure 1: The twelve HadAM grid points analyzed in this study.

three datasets:

- OBS: upscaled daily observations based on over 6000 rain-gauge stations
- HADAM: HadAM3P simulated daily precipitation totals for control climate; indices averaged over the three ensemble members
- NCEP: NCEP daily precipitation interpolated onto the HadAM grid

for the common period 1971–1990.

Seasonal values of the STARDEX indices listed in Table 1 are calculated for every year in the evaluation period.

Table 1: STARDEX indices considered in the present analysis.

name	description
AV	mean precipitation
SDV	standard deviation of daily precipitation
FRE	precipitation frequency
INT	simple daily intensity
Q90	90th percentile of rainday amounts

Results

Following HadAM and NCEP precipitation is evaluated against the upscaled observations as a function of season, index, and spatial location. All seasonal values for each season, index, and grid point are summarized in form of box plots (Fig. 2–6). This allow a direct comparison of the mean values and the magnitude of the interannual variations.

Winter

Mean winter precipitation (AV) is, for both models, generally lower than observed for the southern and eastern-most grid points. For the Alpine (northern, central) grid points the picture is quite different. While NCEP precipitation is generally too low, HadAM precipitation is too high. Very similar results are obtained also for the day-to-day variability (SDV). Looking at FRE and INT, it can be seen that the biases are due to both wrong frequencies and wrong intensities.

Summer

Mean summer precipitation is generally too low for HadAM (except grid point 09) and significantly too high for NCEP. Also the range of interannual variability is rather large for NCEP. The daily variability (SDV) is about as observed for NCEP, but too low for many grid points of HadAM. For NCEP the biases are mainly due to too high precipitation frequencies, while for HadAM the underestimation is a result of both too low frequencies and too low intensities. Note the west-east gradient observed for AV, FRE, and INT for the northern grid points is nicely reproduced by HadAM.

Spring

Mean spring precipitation is relatively close to observations for many grid points for both models. The good performance of NCEP is however partly due to error compensation between too high frequencies and too low intensities. Note that HadAM shows similar error characteristics like in summer, although smaller errors.

Autumn

Mean autumn precipitation is generally too low for NCEP, but close to observations for HadAM. Both models do a good job for precipitation frequency, but precipitation intensity is much too low for NCEP.

Large-scale patterns

The differences between the HadAM and NCEP found in the Alpine region are not untypical (see Appendix). In winter, HadAM is generally wetter than NCEP in central to northern Europe and in the adjacent Atlantic region, and drier in the Mediterranean and some areas in the high latitudes. In summer, there is a marked contrast between continental and oceanic regions. Over the ocean, HadAM is wetter than NCEP, while over land it is much drier than NCEP. The comparison with observations in the Alpine area indicate that NCEP is not necessarily closer to the truth.

Comparsion of HadAM ensemble members

For most indices, seasons and grid points the differences between the three ensemble members are very small. In autumn, however, some of the southern grid points (01, 02, 03) show larger differences for AV, SDV, INT, and Q90. For instance, the 90% quantile of the second member lies outside the inter-quartile range of the other two members for grid point 02.

Conclusion

It has been shown, that the skill of both models varies significantly from region to region, from season to season, and from index to index. The highest skills are obtained for precipitation frequency in autumn and winter (both models), followed by mean precipitation and precipitation intensity in autumn and winter (HadAM). The lowest skills are obtained in summer (both models). From this comparison it can be expected that downscaling using HadAM precipitation should yield at least as good results as using NCEP precipitation.

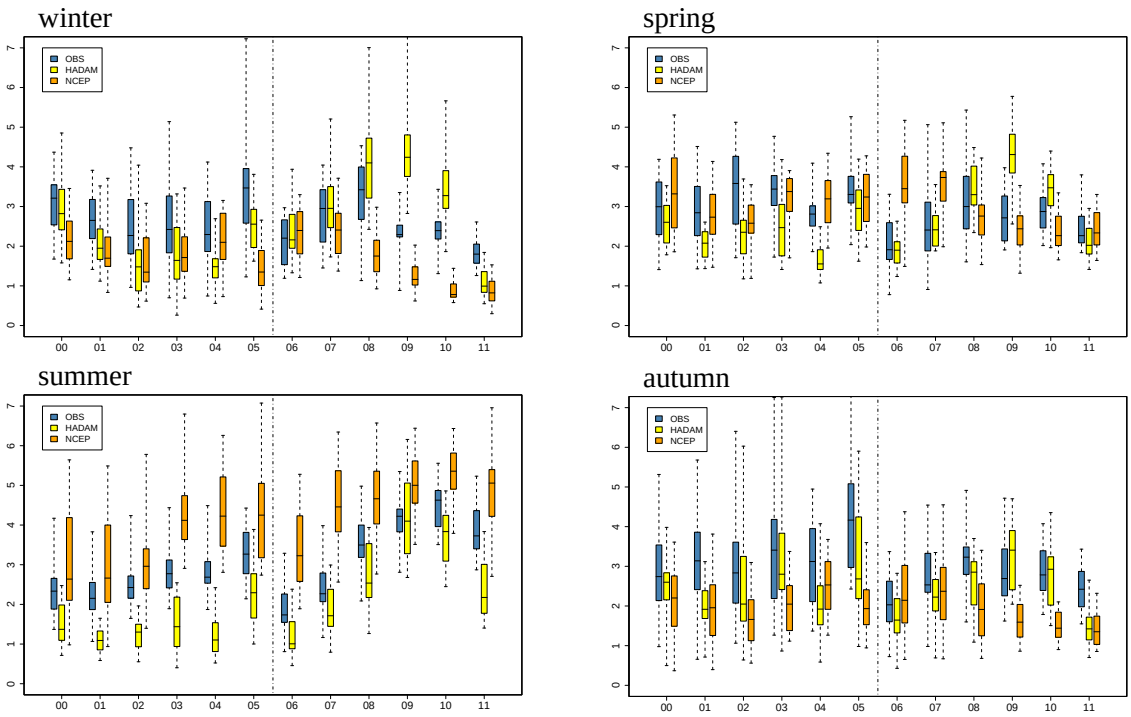

Figure 2: Box plot of the seasonal values of AV for the twelve Alpine grid points

.

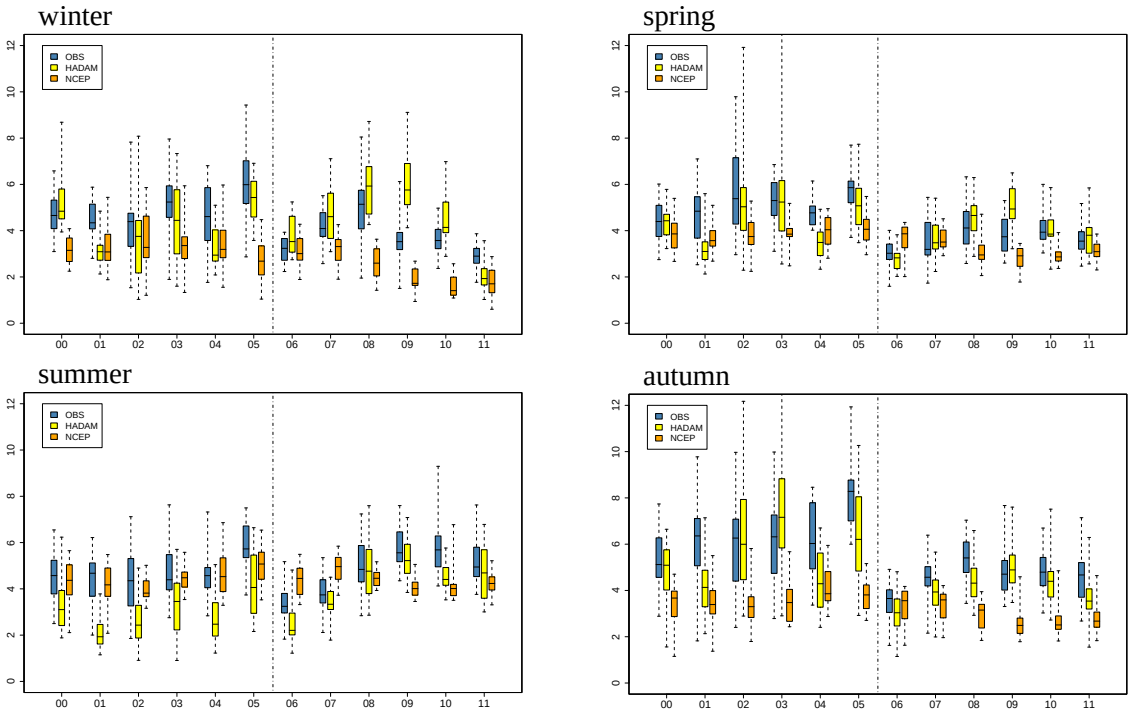

Figure 3: Box plot of the seasonal values of SDV for the twelve Alpine grid points

.

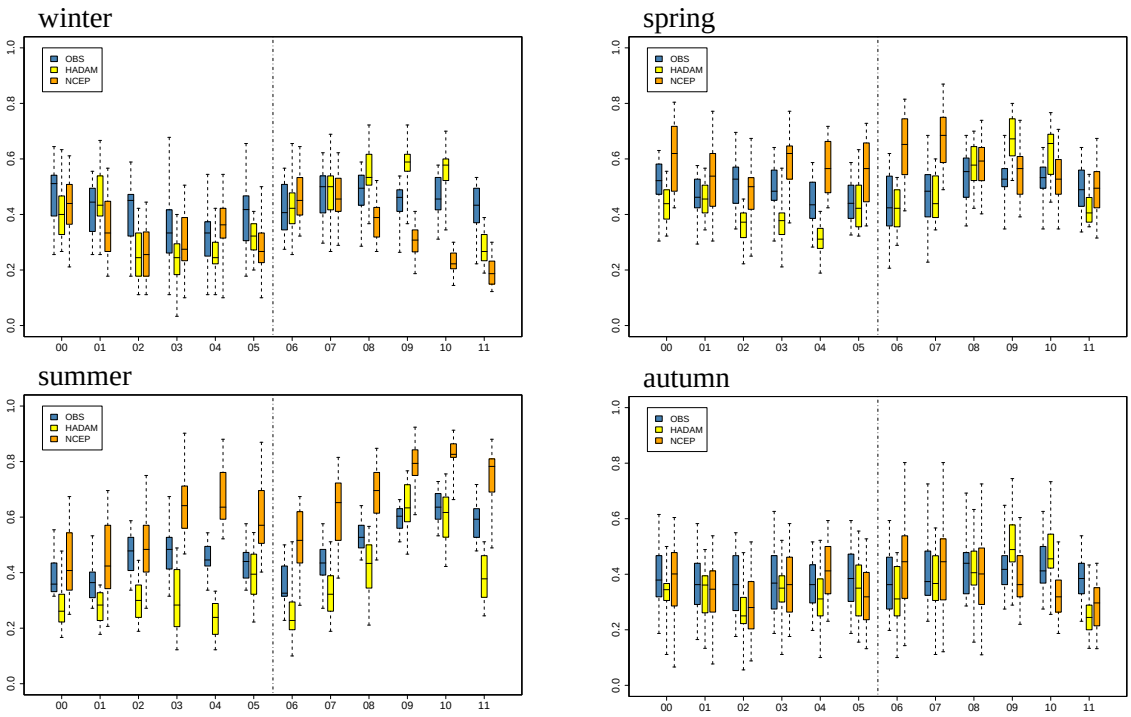

Figure 4: Box plot of the seasonal values of FRE for the twelve Alpine grid points

.

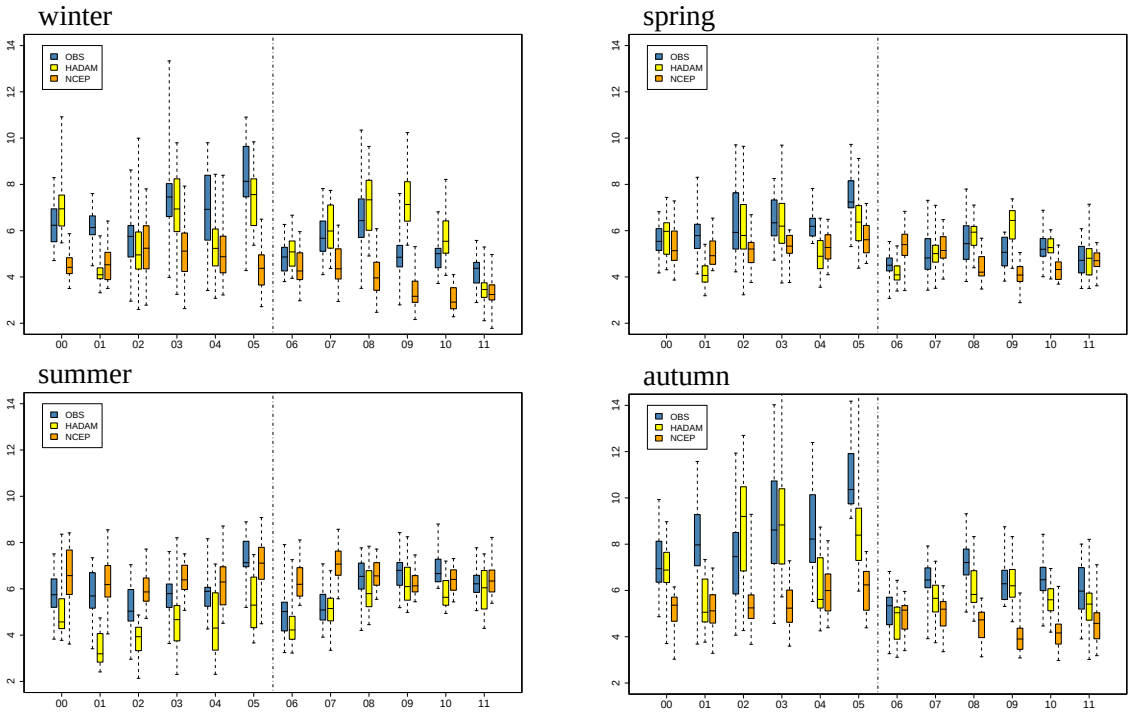

Figure 5: Box plot of the seasonal values of INT for the twelve Alpine grid points

.

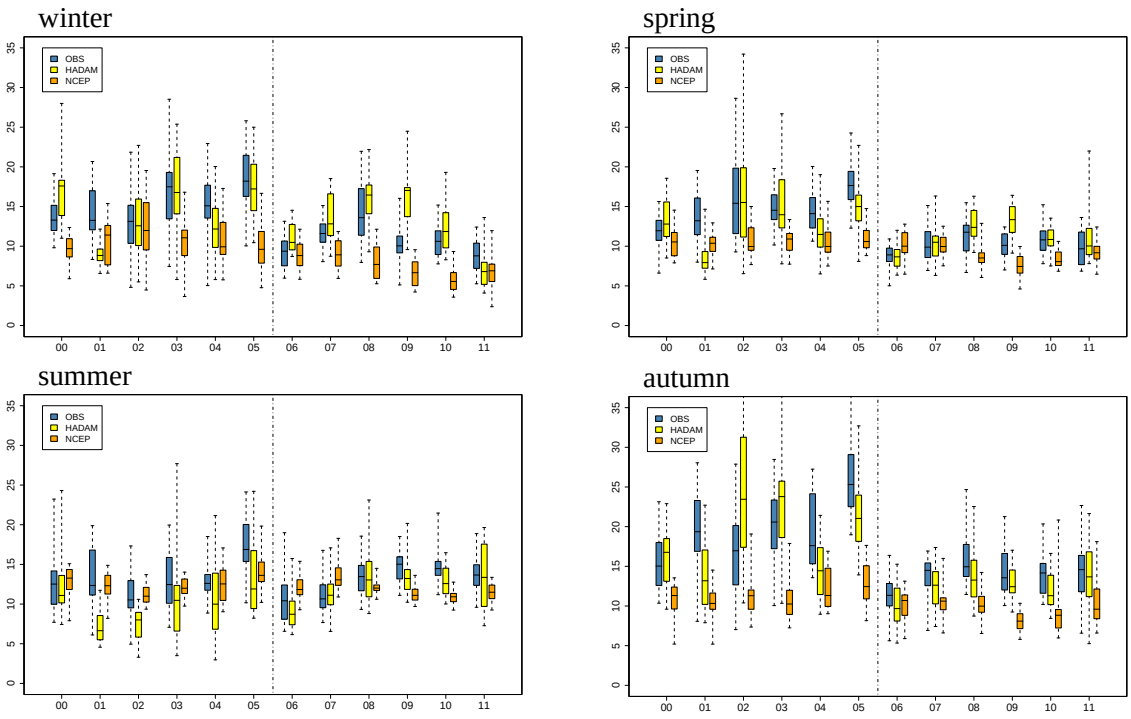

Figure 6: Box plot of the seasonal values of Q90 for the twelve Alpine grid points

.

Appendix
Comparison of large-scale precipitation in NCEP and HadAM

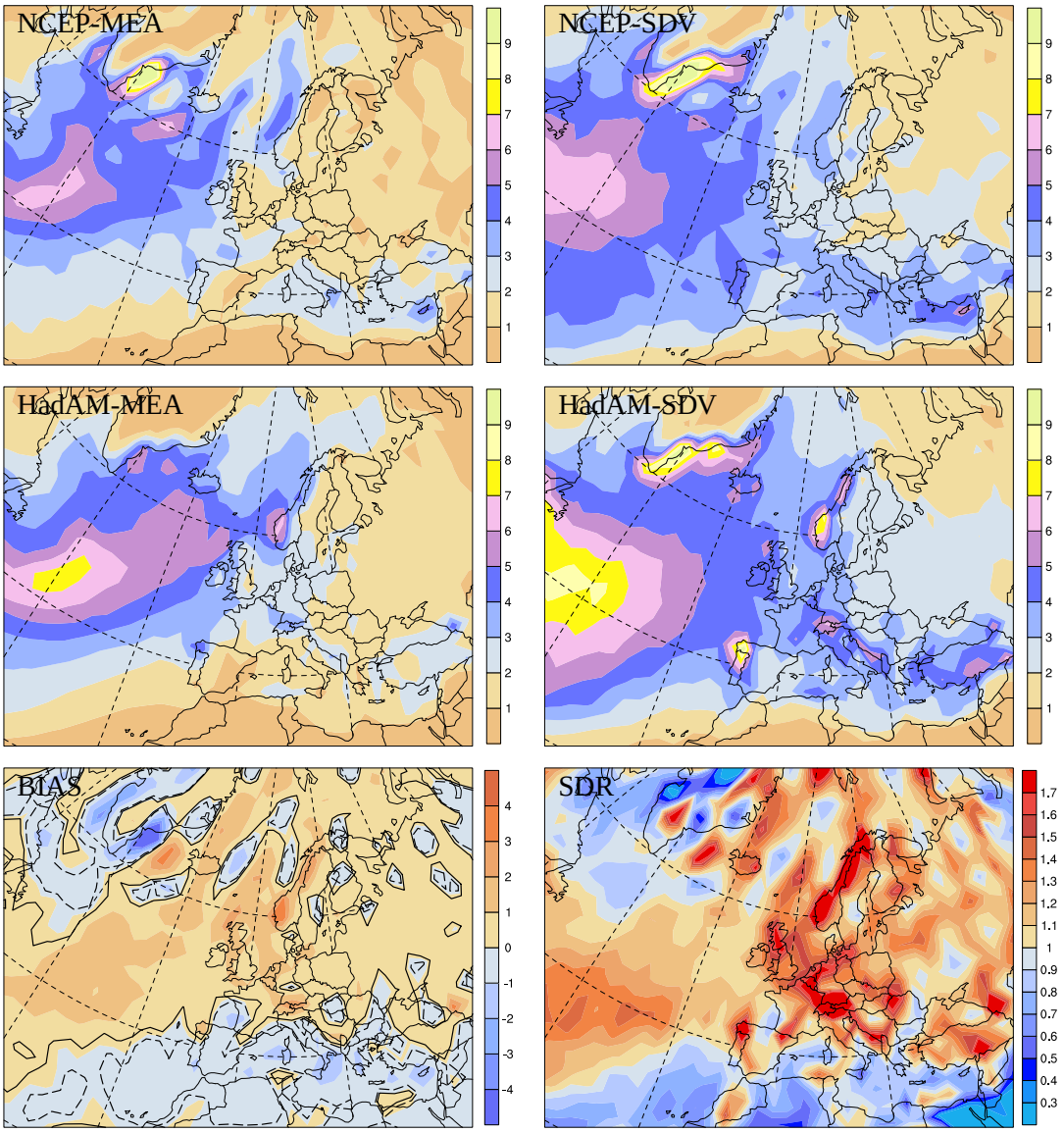

Figure 7: Comparison of NCEP and HadAM precipitation for winter. Top two rows: mean precipitation (MEA) and standard deviation of daily precipitation (SDV). Lowermost row: bias and ratio of the standard deviations.

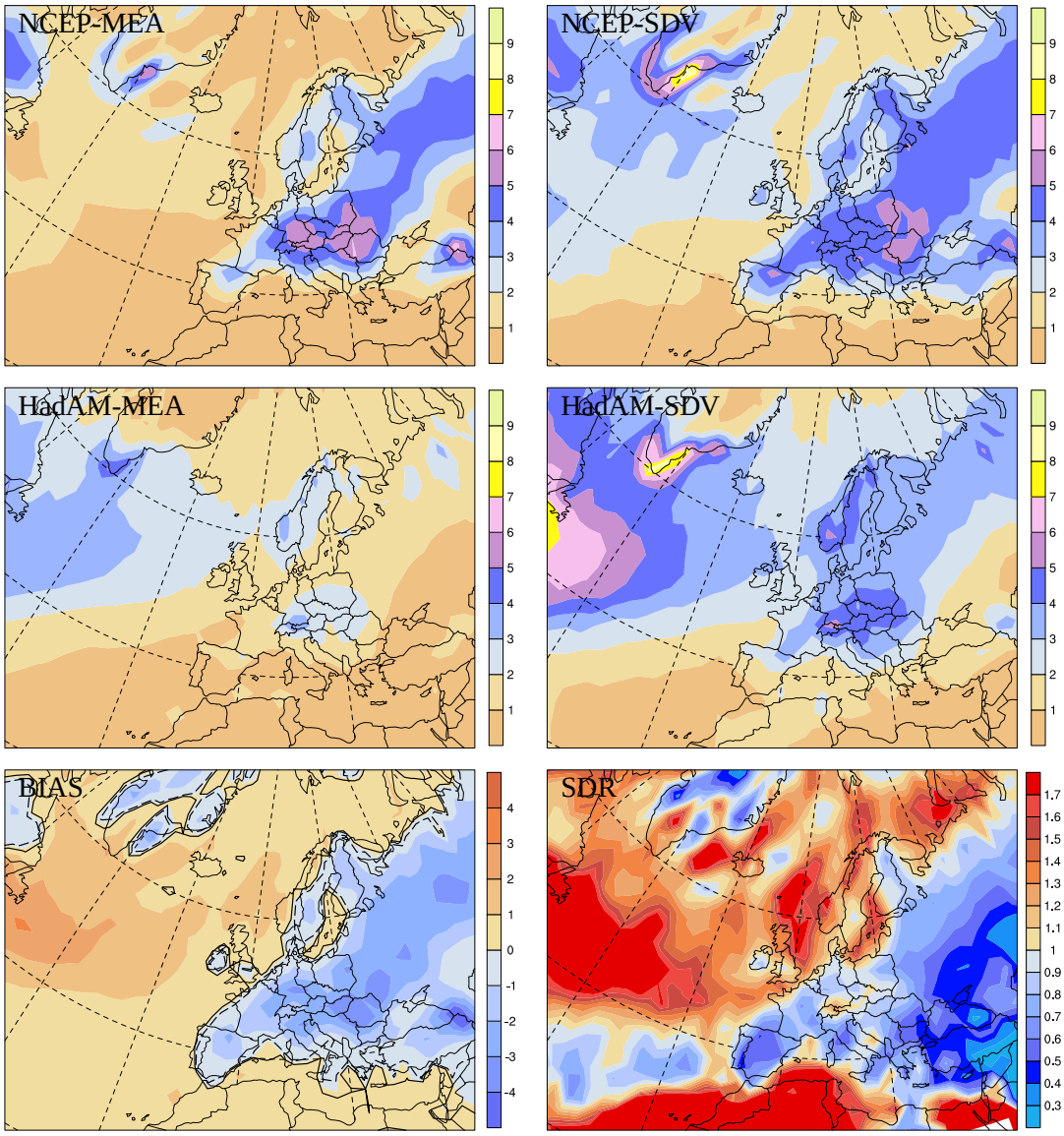

Figure 8: As in Fig.7, but for summer.

Appendix
Comparison of the HadAM3P ensemble members

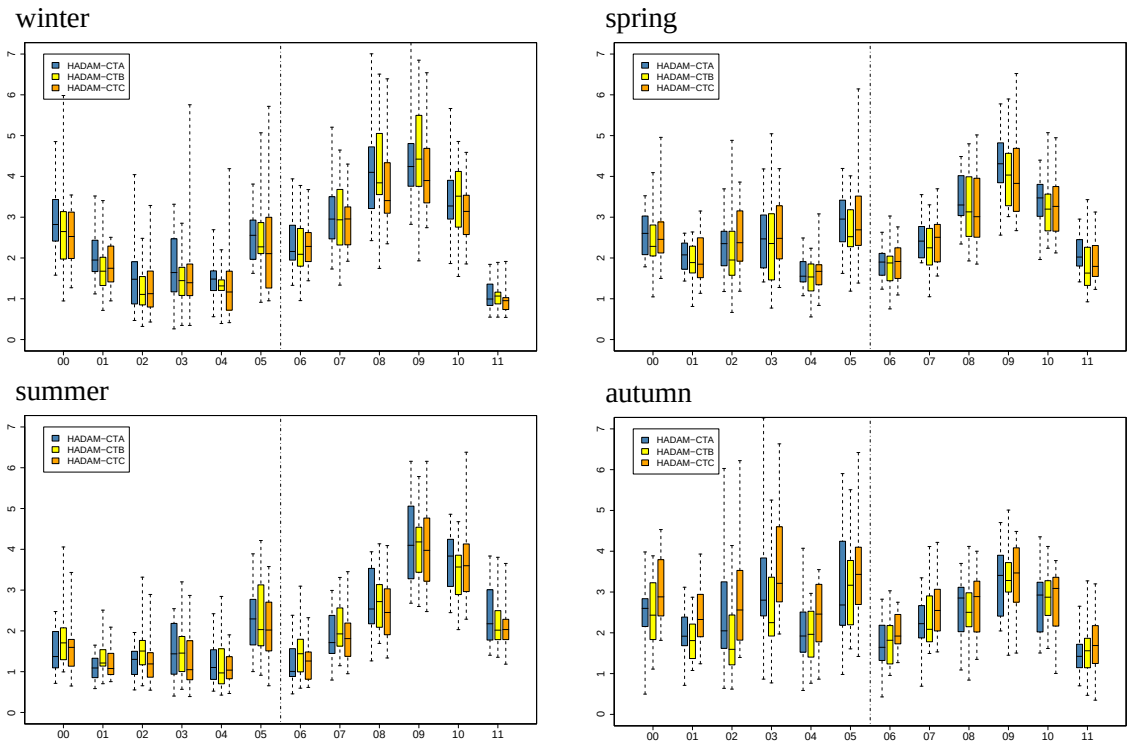

Figure 9: Box plot of the seasonal values of AV for the twelve Alpine grid points

.

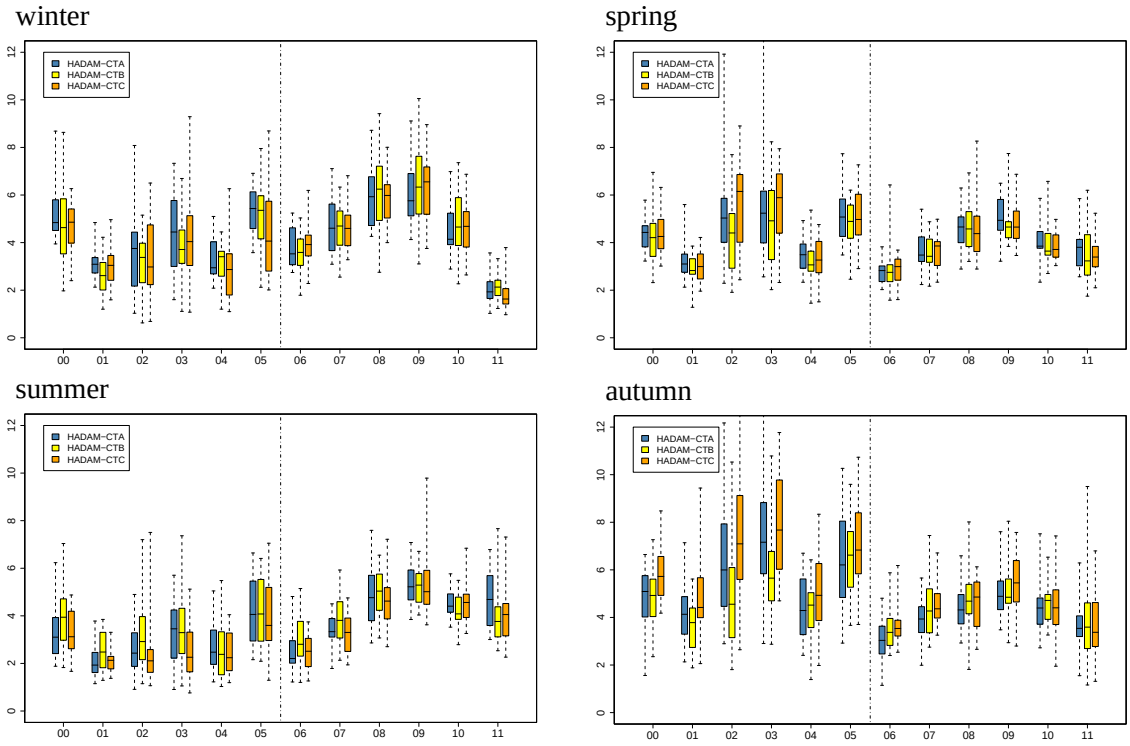

Figure 10: Box plot of the seasonal values of SDV for the twelve Alpine grid points

.

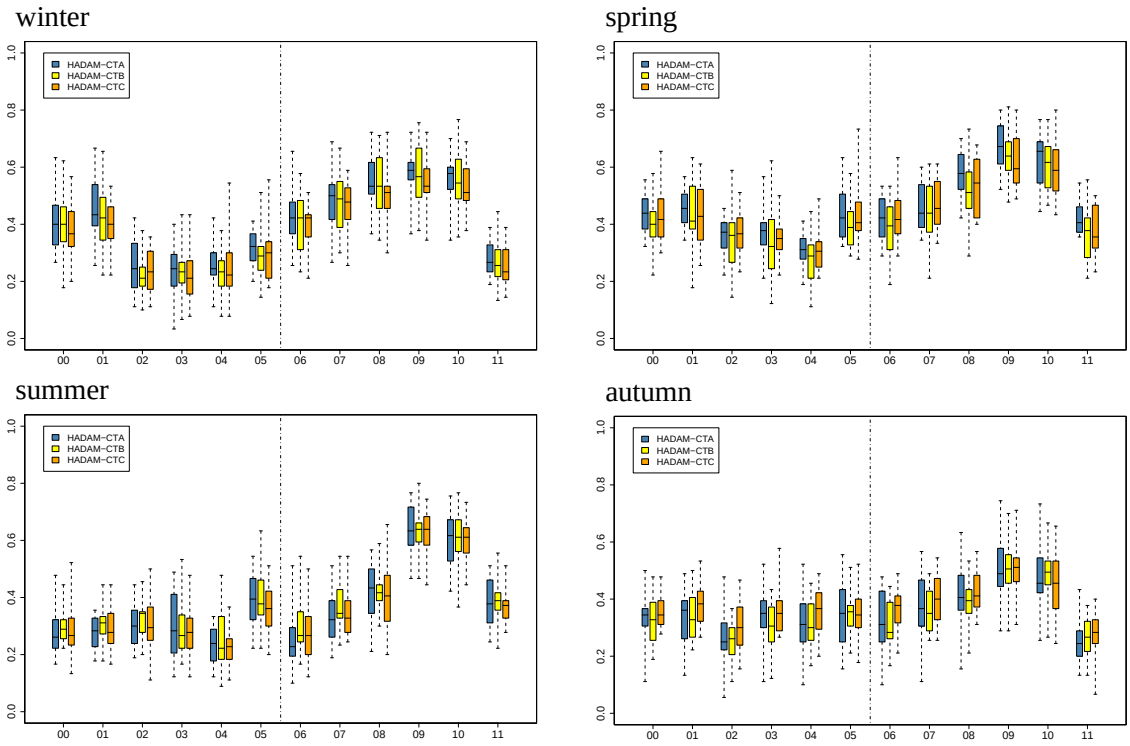

Figure 11: Box plot of the seasonal values of FRE for the twelve Alpine grid points

.

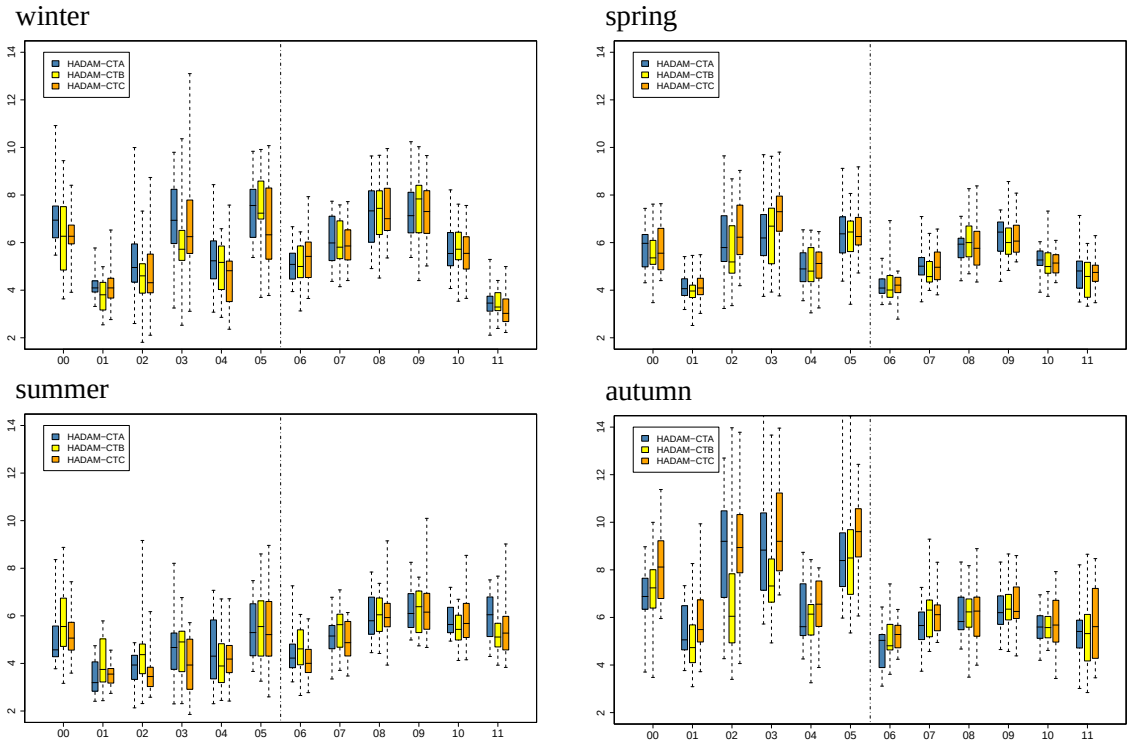

Figure 12: Box plot of the seasonal values of INT for the twelve Alpine grid points

.

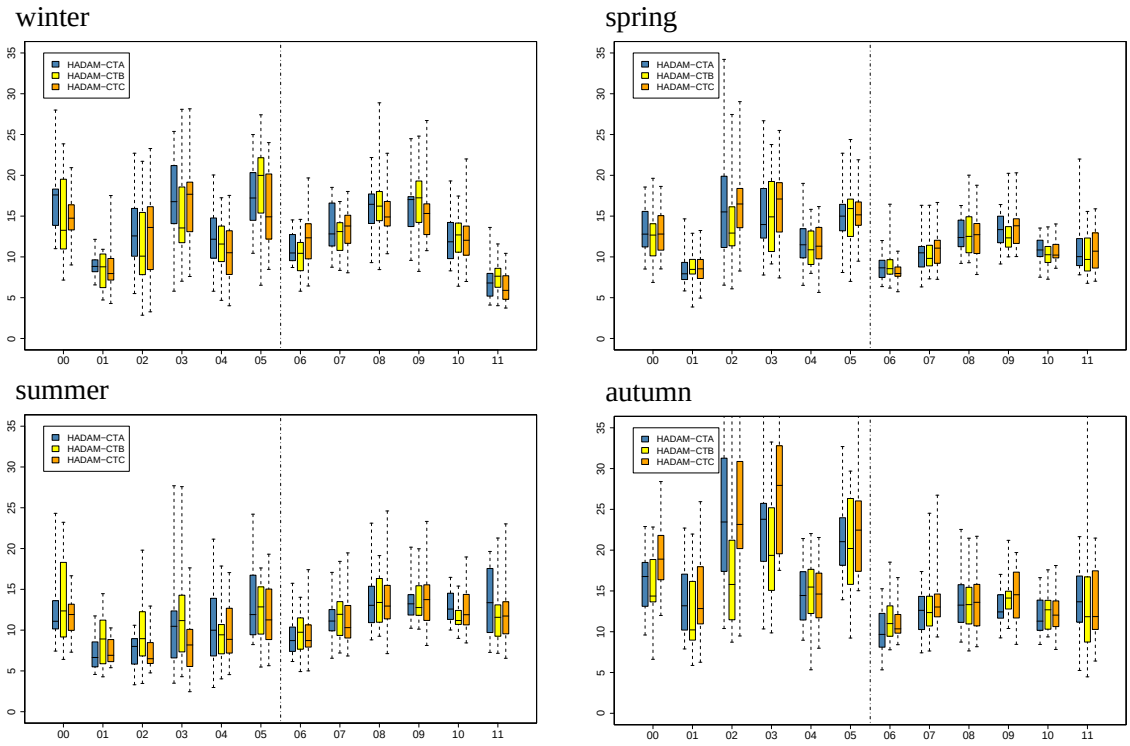

Figure 13: Box plot of the seasonal values of Q90 for the twelve Alpine grid points

.